



ELSEVIER

Contents lists available at ScienceDirect

## Applied Thermal Engineering

journal homepage: [www.elsevier.com/locate/apthermeng](http://www.elsevier.com/locate/apthermeng)

## Research Paper

## Heat transfer correlation of the falling film evaporation on a single horizontal smooth tube



Chuang-Yao Zhao, Wen-Tao Ji, Pu-Hang Jin, Wen-Quan Tao \*

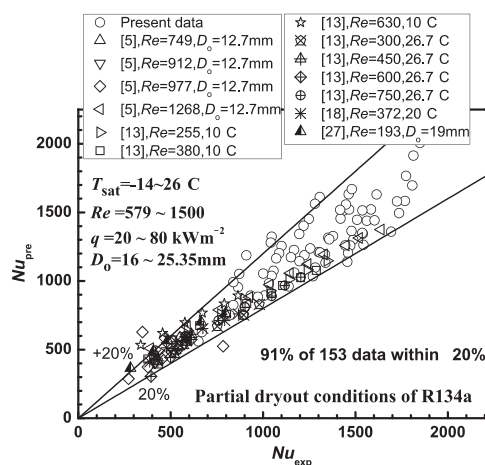
Key Laboratory of Thermo-Fluid Science and Engineering of MOE, School of Energy and Power Engineering, Xi'an Jiaotong University, Xi'an 710049, China

## HIGHLIGHTS

- The effects of tube diameter, saturation temperature, film flow rate and heat flux on heat transfer are studied.
- A threshold Reynolds number is proposed to delineate the test data into full wetting and partial dryout regimes.
- The heat transfer correlations for R134a outside a single horizontal tube are developed.
- Comparisons between the predicted results and the experimental data of other refrigerants in literature are conducted.

## GRAPHICAL ABSTRACT

For the full wetting regime of falling film evaporation on a single horizontal smooth tube, the proposed correlation fits 94% of the data within  $\pm 20\%$ .



## ARTICLE INFO

## Article history:

Received 30 October 2015

Accepted 23 February 2016

Available online 19 April 2016

## Keywords:

Falling film evaporation

Boiling heat transfer

Refrigerant

Single tube

R134a

## ABSTRACT

The falling film heat transfer of R134a outside a single horizontal smooth tube is experimentally investigated, and the effects of the tube diameter, saturation temperature, film flow rate and heat flux are studied. A threshold Reynolds number is proposed to delineate the test data into full wetting and partial dryout regimes. New correlations based on the present data and some data in literature are fitted for both regimes. The correlation for partial dryout regime fits 91% of the 153 data within  $\pm 20\%$ , and the correlation for full wetting regime fits 94% of the 205 data within  $\pm 20\%$ . The correlations have also been compared with previous measured data of other refrigerants available in literature. It is found that the predictions for partial dryout regime agree with most of the previous data with a deviation of  $\pm 30\%$ .

© 2016 Elsevier Ltd. All rights reserved.

\* Corresponding author. Tel/fax: +86 29 82669106.

E-mail address: [wqtao@mail.xjtu.edu.cn](mailto:wqtao@mail.xjtu.edu.cn) (W.-Q. Tao).

## 1. Introduction

Falling film evaporation was early used in the ocean thermal energy conversion (OTEC) systems. In recent decades, it has increasingly attracted attentions in applications of seawater desalination, refinery and petrochemical operation, etc. Falling film evaporation shows great potential to replace the flooded evaporation in vapor-compression refrigeration systems for the advantages of higher evaporative heat transfer coefficient, much less refrigerant charge, and the easiness of lubricant return.

The falling film evaporation process is very complicated due to the multitude of influencing factors [1]. According to the latest review, Fernández-Seara and Pardiñas [2] noted that the previous researches disagree with each other about the effects of parameters, and they pointed out that the applicability of proposed correlations is only limited to very specific test conditions. To the authors' knowledge, even for the simplest situation, i.e., falling film evaporation on a single horizontal smooth tube, such a generally-accepted correlation does not exist.

The following is a brief summary of the previous studies on falling film evaporation on a single smooth tube. (1) The major influencing factors on the heat transfer coefficient are film flow rate, heat flux, saturation temperature and tube diameter [3]; (2) the relationship of heat transfer coefficient with film flow rate can be divided into two distinct stages [4]: a plateau stage with full wetting, and a sharply decreasing stage with partial dryout. Under the premise of full wetting the increase of heat flux always has positive effect on nucleate boiling heat transfer because of the increasing nucleate site density [5]; (3) film flow rate usually has positive effect on the heat transfer coefficient; (4) the effects of the saturation temperature and the tube diameter are diverse, some cases positive and some cases negative [3,5–9]. Further studies are needed in this regard.

Up to now, a large number of correlations have been proposed, but it is difficult to apply these predictions in other environments because of their very specific test conditions [2,3]. The work conducted in References 7,10, and 11 shows that the heat transfer coefficient of falling film heat transfer can be correlated with  $Re$  and  $Pr$ , as for the conventional convective heat transfer process. The first heat transfer correlation for a single tube was probably put forward by Danilova et al. [12], who worked for the evaporator of refrigeration system by using falling film evaporation process. The most recent publication was given by Chien and Chen [13]. The correlations of falling film evaporation published in these publications for a single tube are listed in Table 1.

**Table 1**  
Heat transfer predictions for falling film evaporation on horizontal tube.

	Correlation	Fluid/ $D_o$ , mm	Work condition $q$ , kWm <sup>-2</sup>
[6]	$h_o = 5.169 \times 10^{-11} (rg\rho_l D_o^2) / (\Delta T \mu) (\delta/D_o) (1 + \delta')$	Water/20–40	$Re: 200 \sim 2500$
[8]	$h_o (\nu_l^2/g)^{1/3} / \lambda_l = a Re^{0.10} Pr^{0.65} q^{0.4}$ $8.2 \times 10^{-4}$ for 25.4 mm, $9.4 \times 10^{-4}$ for 50.8 mm	Water/25.4–50.8	$\Gamma: 0.135 \sim 0.366$ kgs <sup>-1</sup> $q: 30 \sim 80$
[12]	$h_o / \lambda_l (\sigma/g(\rho_l \times 10^{-4} \rho_v))^{1/2} = 1.324 \times 10^{-3} (q/r\rho_v \nu_l (\sigma/g(\rho_l - \rho_v))^{1/2})^{0.63} (P_{sat}/\sigma (\sigma/g(\rho_l - \rho_v))^{1/2})^{0.72} Pr^{0.48}$	R-22, R-12 and R-113/18.0	$Re: 135 \sim 2500$ $q: 0.5 \sim 25$
[13]	$h_o = (56.13 We^{0.5878} Re^{0.2457} / Bo^{0.1798}) h_{nb} + h_{cv}$	R134a/19.0	$Re: 184 \sim 750, Pr: 3.45 \sim 3.74, We: 2.3 \sim 2.9 \times 10^{-3}, Bo: 0.042 \sim 0.469$
[14]	$h_o (\nu_l^2/g)^{1/3} / \lambda_l = Re^{0.2} Pr^{0.65} q^{0.4}$	Water/50.8	$\Gamma: 16 \sim 3.79$ cm <sup>3</sup> s <sup>-1</sup> $Pr: 1.3 \sim 3.4$ $q: 30 \sim 80$
[15]	$h_o = h_{nb} + 2h_d L_d / \pi D_o + h_{cv} (1 - 2L_d / \pi D_o)$	–	–
[16]	$h_o = (0.185 + 56.21 We^{0.4531} / (Bo^{0.687} Re^{1.3078})) h_{nb} + h_{cv}$	R-123, R-22 R-11, R-134a, R-141b/12.7–19.5	$Re: 157 \sim 2500$ $Pr: 2.54 \sim 5.9$ $q: 2 \sim 100$
[17]	$h_o = 4200 P_{red}^{0.22} q^{0.38} M^{-0.5} Ra^{0.2} 0.0024 Re^{0.91} + h_{dry} (1 - 0.0024 Re^{0.91})$	R134a/19.05	Partial dryout
[18]	$h_o = (0.0152 We^{0.2833} Re^{1.2536} Bo^{1.1789}) h_{nb} + h_{cv}$	R245fa/19.0	$Re: 115 \sim 372, Pr: 6.26 \sim 7.15, We: 1.65 \sim 16.8 \times 10^{-4}, Bo: 0.044 \sim 0.473$

By carefully analyzing experimental process and data reduction process [19], we believe that for a fundamental research of falling film heat transfer we should first conduct the simplest case: falling film heat transfer outside a horizontal smooth tube. Even for this simplest case the following five factors may affect the test data. First is how to determine the saturation temperature for data reduction. For example, Roques and Thome [4] took the liquid temperature before distributor as the saturation temperature with 0.5 K subtraction. Different practices [5,13,18] will eventually introduce some uncertainty in the determination of the saturation temperature. Second, the horizontality of the tube is another important factor. Third, the uniformity of liquid distribution on the tested tube greatly affects the test results. Fourth, the test tube should have enough length to guarantee the enough tube-side water temperature difference by which the heat transfer rate is determined. Finally all the measurement instruments should have enough accuracy. All the above five aspects will be dealt with carefully in the later presentation.

In this paper, the falling film evaporation outside a single horizontal smooth tube is experimentally studied, and the effects of tube diameter, saturation temperature, film flow rate and heat flux are investigated. The test ranges are: tubes with diameter of 16.0, 19.05 and 25.35 mm, the saturation temperature of 6, 10 and 16 °C, film Reynolds number of 579–2700, and heat flux of 10–170 kWm<sup>-2</sup>. In the following presentation the test system will first be introduced, followed by the test procedure and data reduction method. Then the test results will be presented and comparison is made. Finally some conclusions are presented.

## 2. Experimental facility

The experimental setup is schematically displayed in Fig. 1, from which we can see three circulation loops for refrigerant, hot water and cold water in this system. The detailed description of the three systems can be found in Reference 19.

The evaporator shell is a stainless steel cylinder with an inner/outer diameter of 450/466 mm and an effective length of 1450 mm. The evaporator, condenser and all associated pipes are well insulated by a rubber plastic material with thickness of 40 mm and a layer of aluminum foil.

Special care has been taken to obtain uniform liquid distribution. With the inspiration from the design of Roques and Thome [4], a half tubular overflow box and a guide plate are designed in our liquid distributor, as schematically shown in Fig. 2. The liquid dis-

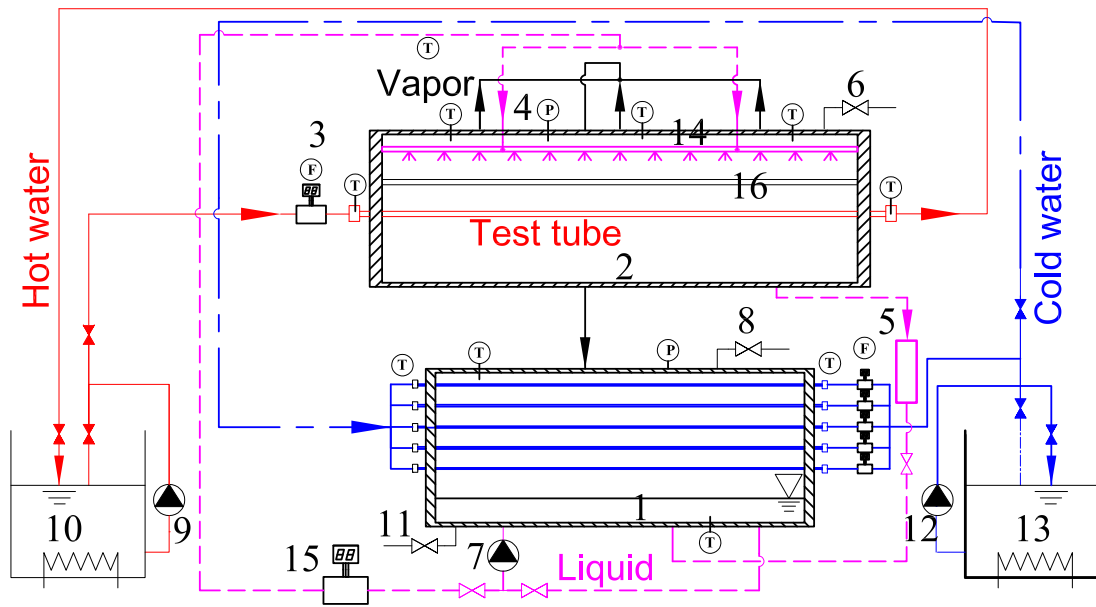


**Fig. 1.** Schematic diagram of the test apparatus. (1) Condenser and refrigerant storage tank; (2) Falling film evaporator and the test section; (3) Electromagnetic flow meter; (4) Pressure gauge; (5) Condensate measuring container; (6) Exhausting valve; (7) Canned motor pump; (8) Refrigerant charging valve; (9) Hot water pump; (10) Hot water tank; (11) Refrigerant outlet; (12) Cooling water pump; (13) Cooling water tank; (14) Liquid distributor; (15) Coliols mass flow meter; (16) Auxiliary distribution tube.

tributor consists of four parts of a multi-perforated pipe, an overflow box, a guide plate and an auxiliary distribution tube. To guarantee the distribution uniformity of the liquid, the pipe has 98 holes drilled in a row, each with a diameter of 2.0 mm and a spacing of 14.0 mm. The liquid distributor, the auxiliary distribution tube and test tube are vertically aligned in an inline arrangement by flanges. During test run, the liquid experiences four times of distribution: the preliminary distribution by the multi-perforated pipes, the readjustment by the overflow box, rectification by the guide plate and momentum reduction by the auxiliary distribution tube, through which the uniformity of liquid distribution can be greatly improved.

The pressure of the system is measured by two pressure gauges (KELLER LEX1) installed at the top and bottom of the evaporator with a range of  $-0.1 \sim 2.0$  MPa and an accuracy of 0.05% of the full scale. The temperatures of refrigerant in the system (including the vapor and liquid phase) are measured and monitored by platinum resistance temperature transducers (Pt100) with an accuracy of  $\pm(0.15 + 0.002|T|)$  K ( $T$  is the tested temperature). The temperatures of the water inlet and outlet are measured by ultra-precise RTD (OMEGA Pt100 1/10 DIN), whose accuracy is  $\pm(0.03 + 0.0005|T|)$  K ( $T$  is the tested temperature). A Keithley digital voltmeter of 0.1 mV resolution is used to measure the electric resistance.

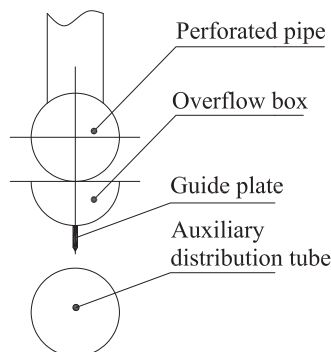


**Fig. 2.** Schematic structure of the liquid distributor.

Three smooth copper tubes with a diameter of 16.0, 19.05 and 25.35 mm and an effective length of 1540 mm are tested in this study. This tube length can provide sufficient temperature difference of the water on tube-side to guarantee the accuracy of the heat transfer rate calculations.

### 3. Experimental procedure and data reduction

#### 3.1. Test procedure

When the installations of the test section have been completed, high-pressure nitrogen is charged into the system, and the internal pressure reaches around 1.2 MPa. The system pressure variation should be less than 1 kPa after 72 hours. If so, the nitrogen is drained, and the system is evacuated by a vacuum pump until the two pressure gauges display no more than 800 Pa (absolute). Then the refrigerant is charged into the system. During this operation, a small quantity of refrigerant is firstly charged and then evacuated by the vacuum pump until the system pressure is again less than 800 Pa. This operation should be repeated three times. After all preparations are completed, appropriate amount of refrigerant is charged into the system.

Before each group of tests, sufficient time is spent to let the system reach an equilibrium condition. The equilibrium condition is identified by the difference between the saturation temperature measured by RTD and the one obtained from REFPROP [20] corresponding to the measured saturation pressure: if it is less or equal to 0.05 K the equilibrium condition is regarded being reached. The acquired data are approved only if the fluctuation of the saturation pressure during the data run is within  $\pm 200$  Pa. A group of data are obtained with decreasing film flow rate at a given heat flux.

The saturation temperature used in data reduction is carefully determined. During tests, we can measure the liquid temperature in the tank of the distributor (the temperature sensor locates near the inlet of the distributor) and the pressure in the system. This liquid temperature in the tank of the distributor is taken as the saturation temperature which is in good agreement with the saturation temperature correspondent to the measured pressure with a

maximum deviation of 0.02 K. The temperature and pressure are strictly maintained at their specified levels during test run, with their fluctuations being controlled within  $\pm 0.02$  K and  $\pm 200$  Pa, respectively.

### 3.2. Data reduction

Because of the good insulation the heat lost in the surrounding is neglected. Hence, the heat balance requirement can be expressed as:

$$(\Phi_e + \Phi_p - \Phi_c)/\Phi \leq 5\% \quad (1)$$

In Eq. (1),  $\Phi_e$  and  $\Phi_c$  are defined as:

$$\Phi_e = \dot{m}_e c_p (T_{e,in} - T_{e,out}) \quad (2)$$

$$\Phi_c = \dot{m}_c c_p (T_{c,out} - T_{c,in}) \quad (3)$$

$\Phi_p$  is the power of the magnetic gear pump (the pump needs cooling during running by using the refrigerant of the system). In the calculation, the properties of water are obtained from Reference 21.  $\Phi$  in Eq. (1) is the reference heat transfer rate, and is defined as follows

$$\Phi = 0.5(\Phi_e + \Phi_c + \Phi_p) \quad (4)$$

The overall heat transfer coefficient of the test tube is described as:

$$k = \frac{\Phi_e}{A_o \Delta T_{LMTD}} \quad (5)$$

where,  $\Delta T_{LMTD}$  is the logarithmic mean temperature difference, defined as:

$$\Delta T_{LMTD} = \frac{T_{e,in} - T_{e,out}}{\ln((T_{sat} - T_{e,out})/(T_{sat} - T_{e,in}))} \quad (6)$$

From thermal resistance analysis, the overall heat transfer coefficient can be expressed as:

$$\frac{1}{k} = \frac{1}{h_i} \frac{D_o}{D_i} + \frac{1}{h_o} + R_w + R_f \quad (7)$$

The fouling thermal resistance  $R_f$  is neglected in the present study because the test tubes had been well cleaned before experiment, the hot water is neat enough and the test is completed in a short time period. The inside convection heat transfer coefficient is determined by Gnielinski equation [21,22],  $h_{gni}$ . The falling film heat transfer coefficient,  $h_o$ , is thus expressed as

$$\frac{1}{h_o} = \frac{1}{k} - \frac{1}{h_{gni}} \frac{D_o}{D_i} - R_w \quad (8)$$

To reduce the uncertainty of the  $h_o$ , the percentage of inside thermal resistance is always kept less than 50%.

The film Reynolds number is determined by

$$Re = \frac{4\Gamma}{\mu} \quad (9)$$

### 3.3. Uncertainty analysis

Uncertainty analysis of the experimental data is conducted along the lines presented in References 23 and 24. The uncertainty of  $k$  for all data is less than 3.2%. The uncertainty of falling film heat transfer coefficient,  $h_o$ , is related to the ones of  $k$  and  $h_i$ . Here the uncertainty of  $h_i$  is estimated by the Gnielinski equation [21,22]

**Table 2**

Experimental uncertainties of measured overall and falling film heat transfer coefficients.

$D_o$ , mm	$T_{sat}$ , °C	$q$ , kWm <sup>-2</sup>	$k$ , kWm <sup>-2</sup> K <sup>-1</sup> $\delta_{max}$	$h_o$ , kWm <sup>-2</sup> K <sup>-1</sup> $\delta_{max}$
16.0	6	20	3.09%	18.33%
		40	3.19%	16.30%
		60	3.19%	13.65%
19.05	6	20	3.19%	15.13%
		40	3.18%	17.31%
		60	3.17%	19.30%
	10	20	3.17%	18.34%
		40	3.11%	15.99%
		60	3.10%	18.32%
	16	20	3.17%	17.80%
		40	3.17%	17.77%
		60	3.10%	16.77%
25.35	6	20	3.10%	18.21%
		40	3.09%	18.32%
		60	3.09%	18.33%
	6	20	3.20%	16.33%
		40	3.18%	18.86%
		60	3.15%	18.58%

whose uncertainty is within 10% [25]. For all experimental data, the percentage of water side thermal resistance varied from 30% to 49.7%. The thus-estimated uncertainties of  $k$  and  $h_o$  are shown in Table 2 for all the experimental data, with the maximum uncertainty being about 20%.

## 4. Results and discussion of the affecting factors

### 4.1. Reliability validation of experimental system

The experiment of film condensation outside a smooth copper tube is firstly conducted in this system. And the results are compared with the averaged Nusselt analytical solution [10]. The comparison shows that the deviations are within  $\pm 10\%$ , indicating the reliability of the experimental system.

### 4.2. Effects of tube diameter

The variations of falling film heat transfer coefficient with film Reynolds number for three tubes are presented in Fig. 3. From these figures, following major features may be noted: (1) For the nine cases tested the variation trends of heat transfer coefficient with liquid Reynolds number  $Re$  are the same: the heat transfer coefficient first remains almost the same and then decreases gradually with the decrease of  $Re$ , and when  $Re$  decreases to a certain value the decrease of  $h_o$  becomes significant; (2) for the present three heat fluxes, 16.0 mm diameter tube always behaves the worst, and this inferiority to other two diameters grows with decrease of heat flux; (3) under the lowest heat flux of 20 kWm<sup>-2</sup> the increase of tube diameter has positive effect on falling film heat transfer; (4) with the increase of heat flux the heat transfer coefficient of 19.05 mm diameter reaches the same level as that of 25.35 mm diameter at  $q = 40$  kWm<sup>-2</sup> and even surpasses it at  $q = 60$  kWm<sup>-2</sup>.

Ribatski and Jacobi [3] pointed out that the overall effect of diameter depends on the amount of the local heat transfer coefficient in the boiling region. We believe that to reveal the effect of tube diameter on the heat transfer coefficient the combined effects of film flow rate and heat flux should be taken into account. The increase of tube diameter indeed extends the length of thermal boundary layer development and the area of liquid impingement, but simultaneously it needs more liquid or lower superheat of tube wall to avoid the film dryout. Namely, at lower heat flux and larger film flow rate, when the tube surface is fully wetted, the increas-

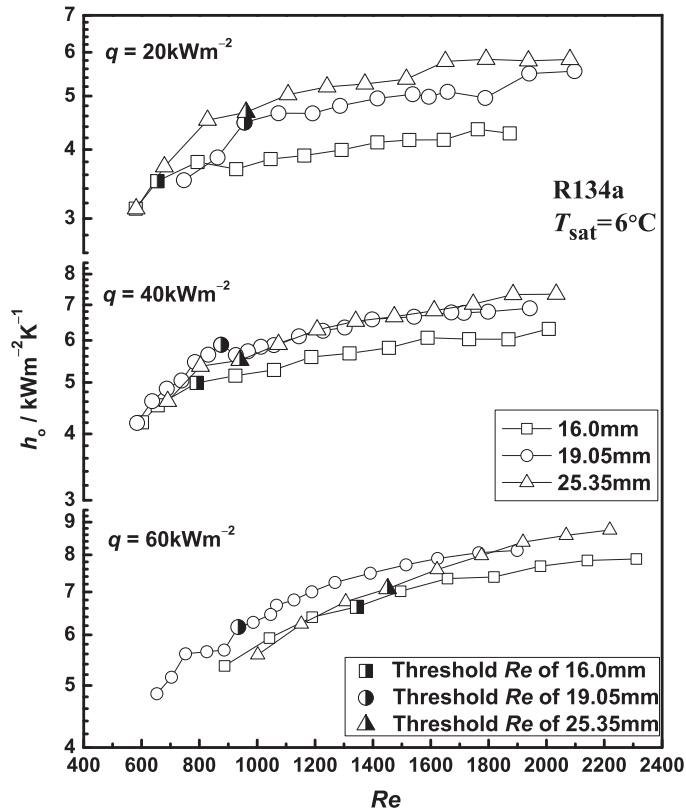


Fig. 3. Falling film heat transfer coefficient of tubes with three diameter and heat fluxes.

ing of tube diameter has positive effect on heat transfer; conversely, at higher heat flux and lower film flow rate, when the tube surface is partial dryout, the increasing of tube diameter has negative effect on heat transfer. Therefore, for the conditions with heat flux of  $20 \text{ kWm}^{-2}$  in the whole film flow rate range,  $40 \text{ kWm}^{-2}$  with  $Re > 1100$  or  $60 \text{ kWm}^{-2}$  with  $Re > 1800$ , a larger diameter is beneficial to heat transfer because there is no film breakdown. However, for the conditions with heat flux of  $40 \text{ kWm}^{-2}$  in the region of  $Re < 1100$  and  $60 \text{ kWm}^{-2}$  in the region of  $Re < 1800$ , the heat transfer performance of 25.35 mm diameter tube is inferior to the 19.05 mm diameter tube. It should be noted that the surface has been well wetted on 16.0 mm diameter tube over the whole range of heat flux and film flow rate in this study.

#### 4.3. Determination of $Re_{\text{threshold}}$

In general, it is difficult to observe whether a tube is working at partial dryout or full wetting conditions. From our experiences and previous studies it can be recognized by comparing the variation of heat transfer coefficients with film flow rate. All our measured experimental curves of  $h_0$  vs.  $Re$ , as shown in Fig. 4, have the same variation trend: with the decrease in film Reynolds number,  $Re$ , the heat transfer coefficients first remain almost the same and then decrease, and when the film Reynolds number decreases to a certain value the decreasing slope becomes sharp. It is here when the flow regime transition occurs: from full wetting to partial dryout. The following strategy is used to find the transition point from full wetting to partial dryout regime:

- (1) For each test case (with fixed diameter, heat flux and saturation temperature, etc.) the test data are arranged in order

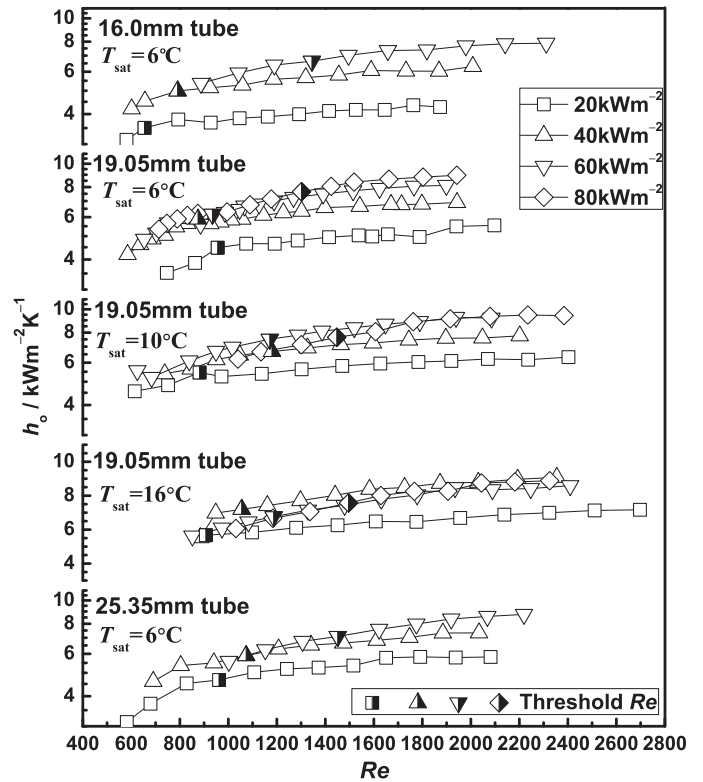


Fig. 4.  $Re_{\text{threshold}}$  determination of eighteen cases.

of the film Reynolds number from the smallest one at the left end to the largest one at right end;

- (2) By observing, taking one film Reynolds number (denoted by  $Re_{\text{try}}$ ) in the region where heat transfer coefficient decreases appreciably with  $Re$ , and averaging the heat transfer coefficients from  $Re = Re_{\text{try}}$  to the largest;
- (3) For the averaged region determining the percentage difference between each local heat transfer coefficient and the averaged data;
- (4) If most percentage differences are much less than 8–10%, then retaking a smaller value of  $Re_{\text{try}}$ ; if most differences are larger than 8–10%, then retaking a larger value of  $Re_{\text{try}}$ , and re-doing the above calculation;
- (5) If the adopted  $Re_{\text{try}}$  can make the largest differences all in the range of 8–10%, then taking this  $Re_{\text{try}}$  as  $Re_{\text{threshold}}$ .

With the help of file EXCEL such calculation can be implemented with ease.

All test data with  $Re$  less than  $Re_{\text{threshold}}$  are regarded in the regime of partial dryout. Such-determined  $Re_{\text{threshold}}$  is shown in Figs. 3–5 by special symbols.

#### 4.4. Effect of saturation temperature

For four heat fluxes, the effects of temperature are plotted in Fig. 5. From these figures, it can be seen that the effects of saturation temperature have the following features. At lower heat fluxes of 20 and  $40 \text{ kWm}^{-2}$ , the increase of saturation temperature promotes the heat transfer in the entire range of film flow rate, and the highest heat transfer coefficient occurs at the highest saturation temperature ( $16^\circ\text{C}$ ). While at higher heat fluxes of 60 and  $80 \text{ kWm}^{-2}$  the differences of heat transfer coefficients under different saturation temperatures gradually decrease. In addition, the highest heat

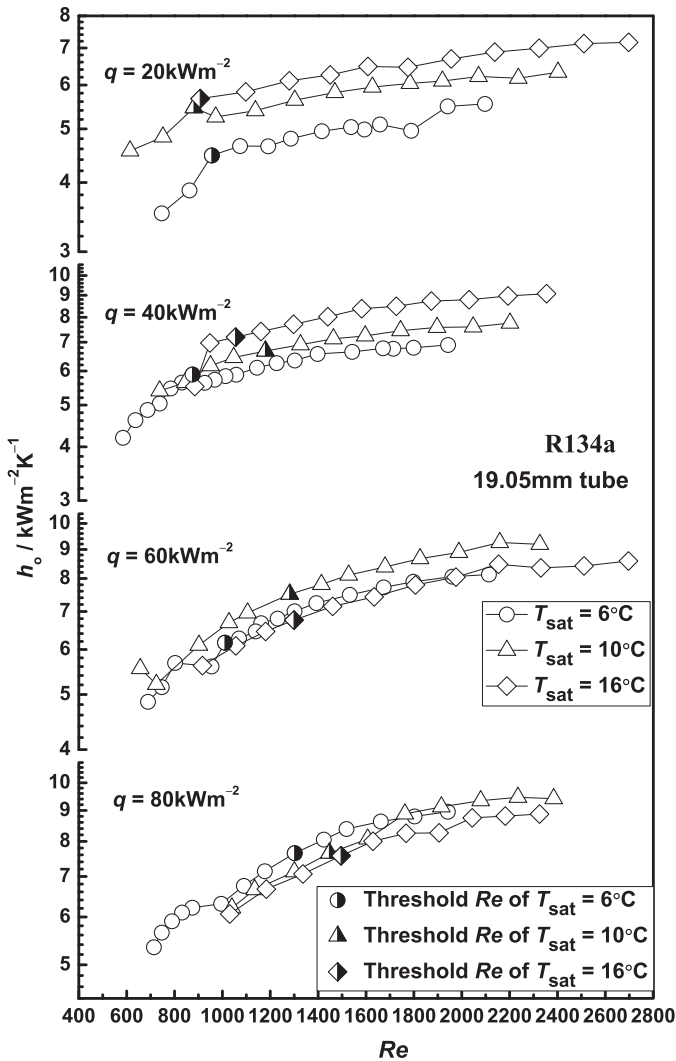


Fig. 5. Effect of saturation temperature on falling film heat transfer coefficient for four heat flux.

transfer coefficient occurs at 10 °C for heat flux of 60 kWm<sup>-2</sup> and at 6 °C for heat flux of 80 kWm<sup>-2</sup>.

The above results may be resulted from the following reasons. On one hand, the increase of saturation temperature decreases the liquid viscosity, hence, decreases the film thickness, and the falling down of liquid from the tube bottom also becomes easier. On the other hand, the decrease of the liquid viscosity and film surface tension with the increase in saturation temperature would make the film breakdown easier by the generated bubbles in the film, which would deteriorate the falling film heat transfer. The results shown in Fig. 5 are the outcome of the balance between the two contradictory factors.

#### 4.5. Effects of film flow rate and heat flux

From above presentation, a general trend of heat transfer coefficient can be observed for a specified heat flux condition along the descending film flow rate direction. At the larger film flow rate region, the decrease in heat transfer coefficient with the decrease in film flow rate is mild, and when the film flow rate descends to a certain value a significant decrease in the heat transfer coefficient occurs. This phenomenon can be regarded as the breakdown of liquid film, i.e., the occurring of partial dryout.

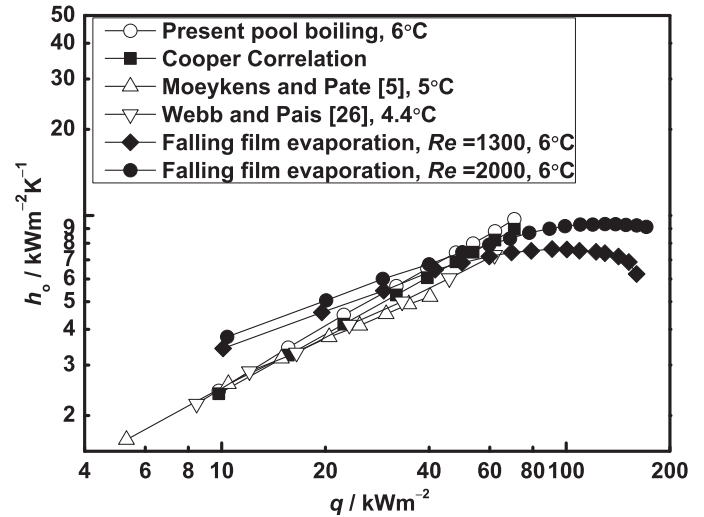


Fig. 6. Effect of heat flux on falling film coefficient.

In order to reveal the effect of heat flux special tests are conducted. In these tests the film flow rate and the saturation temperature are fixed. The falling film evaporation heat transfer coefficients of 19.05 mm diameter tube under two film flow rates vs. the heat flux are displayed in Fig. 6, where the measured pool boiling heat transfer coefficient in References 5 and 26 and the one measured by the present authors are also presented. For a comparison purpose the predicted values by Cooper equation [27] are also shown. As can be seen there, with the increase of heat flux the heat transfer coefficient increases almost linearly in the test range of heat flux, reaches its peak, and then decreases because of gradually increase of dry patches area. Within the high heat flux region the decrease trend of heat transfer coefficient at lower film Reynolds number case (=1300) is more significant than the higher film Reynolds number case (=2000). From the figure we can see that the variation slope of  $h_o$  vs.  $q$  of pool boiling is larger than that of falling film evaporation. For the cases studied at  $q \approx 40$  kWm<sup>-2</sup> the three curves cross each other, below which the heat transfer performance of falling film evaporation is higher than the pool boiling.

## 5. Heat transfer correlation for single smooth tube

### 5.1. Dimensional analysis

First the dimensional analysis method is adopted to obtain the related dimensionless numbers for the falling film heat transfer. According to the present experimental conditions the heat transfer coefficient  $h_o$  could be influenced by heat flux  $q$ , film flow rate  $\Gamma$ , liquid viscosity  $\mu_l$ , liquid thermal conductivity  $\lambda_l$ , latent heat  $r$ , surface tension  $\sigma$ , and liquid specific heat capacity  $c_p$ . The external force driving the liquid flow is gravity, represented by the gravitational acceleration  $g$ , and the refrigerant density difference,  $\rho_l - \rho_v$ , may induce some buoyancy effect. The tube outside diameter  $D_o$  is the major characteristic dimension of the test system.

From the dimensionless analysis, we can obtain following well-known dimensionless criteria:

$$\text{Nusselt number } Nu = h_o D_o / \lambda_l;$$

$$\text{film Reynolds number } Re = 4\Gamma / \mu_l;$$

$$\text{Prandtl number } Pr = \mu_l c_p / \lambda_l;$$

$$\text{Boiling number } Bo = q D_o / r \Gamma;$$

$$\text{Modified Weber number } We = \frac{\Gamma^2}{\pi^2 (\rho_l - \rho_v) D_o \sigma};$$

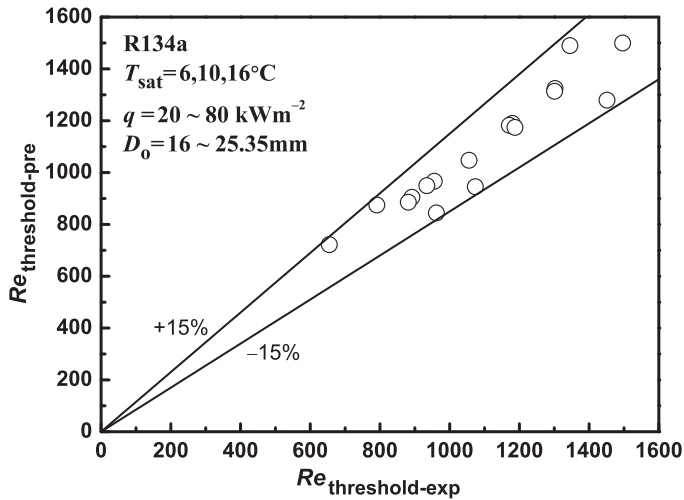


Fig. 7. Comparison of  $Re_{\text{threshold}}$  between prediction and test data.

and Archimedes number  $Ar = gD_o^3/\nu_f^2$ .

Since the experiments are performed at the constant gravitational field, the Archimedes number related to gravity effect is neglected.

### 5.2. Strategy of correlating test data

Considering the general trend of the heat transfer coefficient along with the decreasing of film flow rate, correlations are constructed for two regimes: partial dryout and full wetting conditions. We classify the data of the two regimes by using the method proposed in Section 4.3.

The data of all test cases are depicted together in Fig. 4. As displayed in this figure, the transition film Reynolds number varies with heat flux, saturation temperature and tube diameter. For all our test cases this transition Reynolds numbers can be correlated by the following correlation:

$$Re_{\text{threshold}} = C_1 Bo^{a_1} Pr^{a_2} We^{a_3} \quad (10)$$

The values of  $C_1$  and  $a_1 \sim a_3$  are obtained using regression analysis:

$$\begin{aligned} C_1 &= 5.36 \times 10^4, \\ a_1 &= 0.45 \times 10^{-2}, \\ a_2 &= -0.52, \\ a_3 &= 0.50. \end{aligned}$$

The comparison of the predicted  $Re_{\text{threshold}}$  with test data is shown in Fig. 7 with the maximum deviation of 15%.

### 5.3. Correlations of the two regimes

To enlarge the range of the test parameters, some experimental data of the falling film evaporation of R134a outside a single horizontal tube in the literature are correlated together with the present data based on the above dimensionless criteria. All data in the literature are firstly identified their working regimes (partial dryout or full wetting) based on Eq. (10). The adopted previous studies are from References 5,13,18, and 28. Totally 153 and 205 test data are adopted from the figures of their published papers for the partial dryout and full wetting regimes, respectively.

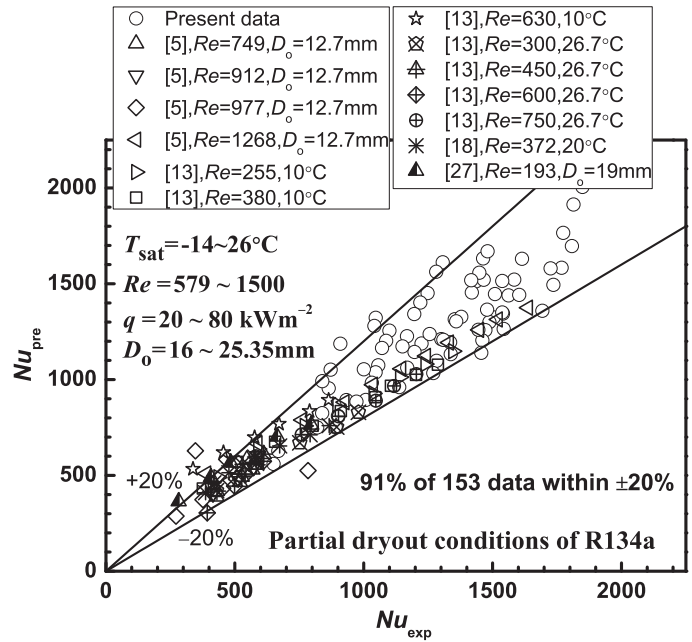


Fig. 8. Comparison between predicted heat transfer coefficient and based experimental data for partial dryout regime.

The correlations of the two regimes are proposed as follows:

$$Nu = C_2 Re^{b_1} Bo^{b_2} Pr^{b_3} We^{b_4} \quad (11)$$

The characteristic temperature for determining the thermophysical properties is the saturation temperature.

By using regression analysis the values of  $C_2$  and  $b_1 \sim b_4$  are obtained. The resulted correlation for the partial dryout regime is:

$$Nu = 4.64 \times 10^{-3} Re^{1.51} Bo^{0.43} Pr^{0.15} We^{-0.45} \quad (12)$$

$$\begin{aligned} Re: & \text{from } 255 \text{ to } 1495, \\ Bo: & \text{from } 0.42 \times 10^{-2} \text{ to } 21.4 \times 10^{-2}, \\ Pr: & \text{from } 3.40 \text{ to } 4.25, \\ We: & \text{from } 0.93 \times 10^{-4} \text{ to } 45.13 \times 10^{-4}; \end{aligned}$$

and for the full wetting regime it is:

$$Nu = 3.58 \times 10^{-9} Re^{2.89} Bo^{0.37} Pr^{0.2} We^{-1.13} \quad (13)$$

$$\begin{aligned} Re: & \text{from } 250 \text{ to } 2697, \\ Bo: & \text{from } 0.52 \times 10^{-2} \text{ to } 25.88 \times 10^{-2}, \\ Pr: & \text{from } 3.56 \text{ to } 3.83, \\ We: & \text{from } 0.82 \times 10^{-4} \text{ to } 99.58 \times 10^{-4}. \end{aligned}$$

It is worth noting that since the variation ranges of Prandtl number are very limited for both partial dryout and full wetting regimes, so the exponents of Prandtl number in Eqs. (12) and (13) are pre-specified based on referencing previous correlation with try-and-error practices.

The comparisons of the predictions from the proposed correlation with the based experimental data are shown in Figs. 8 and 9 for partial dryout and full wetting regimes, respectively. The deviations are as follows: 91% of 153 data are within  $\pm 20\%$  for the partial dryout regime, and 94% of 205 data are within  $\pm 20\%$  for full the wetting regime.

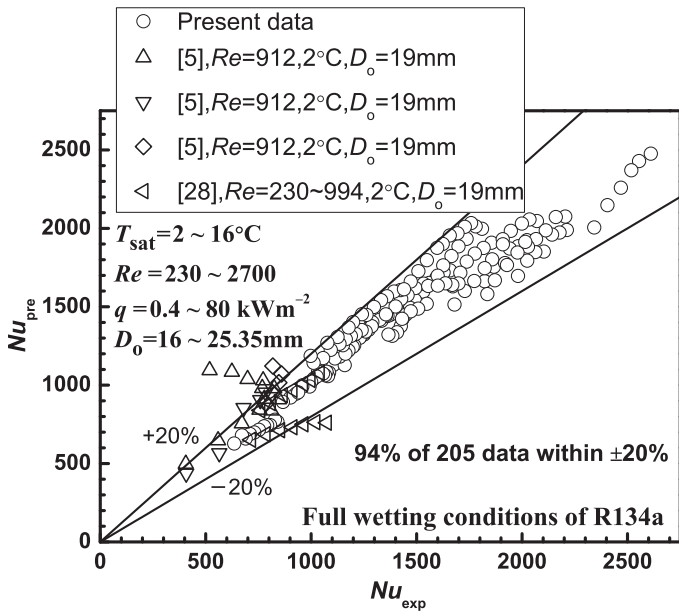


Fig. 9. Comparison between predicted heat transfer coefficient and based experimental data for full wetting regime.

5.4. Comparison with other test data and further research needs

In this section, the data of other investigations for other refrigerants under the similar working conditions are compared with the present correlations. According to Eq. (10) these data are classified into two regimes. Figs. 10 and 11 depict the comparisons between the predicted Nusselt numbers by Eqs. (12) and (13) and the experimental results in literature with refrigerants R123 [28], R22 [12,28], R245fa [18], R11 [29–31], R113 [32] and R141b [33] on a smooth tube for the partial dryout and full wetting regime, respectively. It can be seen from these figures that one data symbol represents one test case with specified refrigerant and saturation temperature. The scopes of the entire data points are:  $Pr=2.44\sim 6.26$ ,  $D_o=18.0\sim 25.0\text{ mm}$ ,  $Re=100\sim 4110$ , and  $q=0.98\sim 90\text{ kWm}^{-2}$ . As ob-

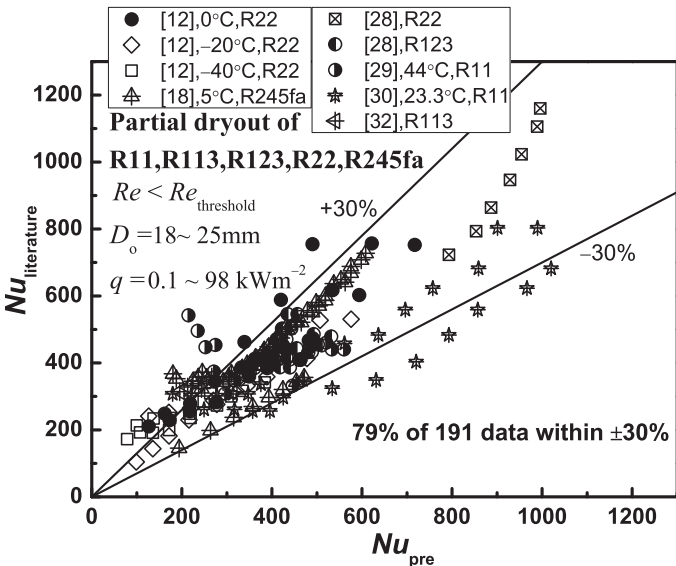


Fig. 10. Comparison of present correlations with previous investigation on other refrigerants for partial dryout regime.

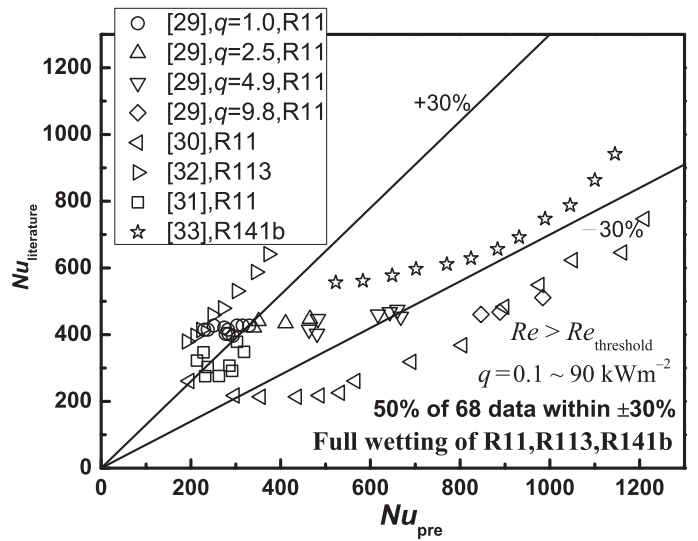


Fig. 11. Comparison of present correlations with previous investigation on other refrigerants for full wetting regime.

served in these figures, the correlations can predict 79% of 191 data of partial dryout case with the deviations of  $\pm 30\%$ , while 50% of the total 68 data of full wetting with the deviations of  $\pm 30\%$ . The agreement for the data of partial dryout is quite satisfactory.

For the full wetting case the agreement between our prediction and test data is much worse. Some preliminary analyses for the reasons are as follows. First, Eq.(10) for determining  $Re_{\text{threshold}}$  may not be applicable to all the test data in other references. As shown in Section 4.3, the values of our  $Re_{\text{threshold}}$  is determined from a continuous variation curve of  $h_o$  vs.  $Re$ , however, in the most previous studies such continuous variation curves were very limited, instead, only a short variation range of  $Re$  vs.  $h_o$  was figured. Whether the value determined by Eq. (10) is applicable to such case needs further validation. Second, some test data were provided without detailed description of how to determine the saturation temperature, which may also introduce a certain deviations. Third, the relatively large measurement uncertainty of falling film evaporation heat transfer coefficients may be one of the reasons. As for the results measured by the group of Thome [4,17,34], they are also compared with the present correlations, but the divergences are more than 100% for both partial dryout and full wetting cases. One reason for this great divergence may be resulted from the different methods of determination of the saturation temperature. According to our estimation the deviation in heat transfer coefficient caused by adding 0.5 K may result in about 20% difference, depending on cases. Since for both the partial dryout and full wetting such big deviations exist, while our correlation for partial dryout agrees well with many test data in other references, thus the data from Thome’s group are temporary not included.

As indicated above, the falling film evaporation process is very complicated due to the multitude of influencing factors, and the big deviations for the full wetting case may be regarded as a reflection of such complexity. Some influencing factor(s) may not have been revealed. Although our study make a step forward in this regard in terms of the correlation for the partial dryout case agrees with test data quite well, further researches are highly required to fully understand the whole process. In this regard the following studies are especially valuable: (1) further verify Eq. (11) for other refrigerants; (2) examine the applicability of Eq. (10) and further improve it; (3) carefully evaluate and examine the previous test data in literature and determine their feasibilities; (4) examine the effect of tube length on the test results under the condition of measure-

ment accuracy. The first three items are now underway at the authors' group.

Reliable data accumulation is very important in order to establish a well-published general correlation. Our test data of this paper will be uploaded in our group website once this paper is accepted. And we appeal other researchers to do so in order to avoid the additional reading errors from paper figures.

## 6. Conclusions

Based on the present study the following conclusions can be drawn:

1. The effect of tube diameter on heat transfer may be positive or negative depending on the levels of the heat flux and film flow rate.
2. The effect of saturation temperature on heat transfer is positive at lower heat flux but negative at higher heat flux.
3. A threshold Reynolds number is proposed to delineate the test data into full wetting and partial dryout regimes. This Reynolds number is based on observing the variation trend of the falling film heat transfer coefficient with the film flow rate at the fixed heat flux. Based on these data a prediction correlation for the threshold Reynolds number is proposed.
4. Two correlations for R134a are constructed based on the test data of ours and references. The correlation for partial dryout regime fits 91% of the total 153 data of R134a within  $\pm 20\%$  while fits 79% of the total 191 data of other refrigerants within  $\pm 30\%$ , and the correlation for full wetting regime fits 94% of the total 204 data of R134a within  $\pm 20\%$  while fits 50% of the total 68 data of other refrigerants within  $\pm 50\%$ .

## Acknowledgement

This work was supported by the National Key Basic Research Program of China (973 Program) (2013CB228304) and the Research fund for National Natural Science Foundation of China (51306140)

## Nomenclature

$A$	Area, $m^2$
$Ar$	Archimedes number, $Ar = D_o^3 g / \nu^2$
$Bo$	Boiling number, $Bo = q D_o / r \Gamma$
$c_p$	Specific heat capacity, $J kg^{-1} K^{-1}$
$D$	Diameter of tube, mm
$g$	Gravity acceleration, $ms^{-2}$
$h$	Heat transfer coefficient, $Wm^{-2}K^{-1}$
$k$	Overall heat transfer coefficient, $Wm^{-2}K^{-1}$
$L$	Tested length of tube, m
$\dot{m}$	Mass flow rate, $kg s^{-1}$
$Nu$	Nusselt number, $Nu = h_o D_o / \lambda_i$
$Pr$	Prandtl number, $Pr = \mu_i c_p / \lambda_i$
$P$	Pressure, Pa
$P_{red}$	The ration saturation pressure to the critical pressure
$q$	Heat flux, $Wm^{-2}$
$R$	Thermal resistance, $m^2 kW^{-1}$
$Ra$	Arithmetical mean deviation of the profile ISO 4287/1:1984 ( $\mu m$ )
$r$	Latent heat, $J kg^{-1}$
$Re$	Film Reynolds number, $Re = 4I / \mu_i$
$T$	Temperature, $^{\circ}C$
$We$	Modified Weber number, $We = \Gamma^2 / (\pi^2 (\rho_l - \rho_v) D_o \sigma)$

## Greek

$\delta$	Film thickness, m
$\theta$	Peripheral angle, degree

$\Gamma$	Liquid film flow rate on one side of the tube per unit length, $kgm^{-1}s^{-1}$
$\Phi$	Heat transfer rate, W
$\lambda$	Thermal conductivity, $Wm^{-1}K^{-1}$
$\mu$	Dynamic viscosity, $kgm^{-1}s^{-1}$
$\nu$	Kinematic viscosity, $m^2s^{-1}$
$\rho$	Density, $kgm^{-3}$
$\sigma$	Surface tension, $Nm^{-1}$
$\Delta$	Variable differential

## Subscript

c	Condensing
e	Evaporating
f	Fouling
v	Gas refrigerant
l	Liquid refrigerant
LMTD	Logarithmic mean temperature difference
i	Inside of tube
in, out	Inlet, outlet
o	Outside of tube
p	Pump
sat	Saturation
w	Wall

## References

- [1] J.R. Thome, Falling film evaporation: state-of-the-art review of recent work, *J. Enhanced Heat Transfer* 6 (1999) 263–277.
- [2] J. Fernández-Seara, Á.Á. Pardiñas, Refrigerant falling film evaporation review: description, fluid dynamics and heat transfer, *Appl. Therm. Eng.* 64 (2014) 155–171.
- [3] G. Ribatski, A.M. Jacobi, Falling-film evaporation on horizontal tubes – a critical review, *Int. J. Refrig.* 28 (2005) 635–653.
- [4] J.F. Roques, J.R. Thome, Falling films on arrays of horizontal tubes with R-134a, part I: boiling heat transfer results for four types of tubes, *Heat Transfer Eng.* 28 (2007) 398–414.
- [5] S.A. Moeykens, M.B. Pate, Spray evaporation heat transfer of R-134a on plain tubes, *ASHRAE Trans.* 100 (1994) 173–184.
- [6] L. Xu, M.R. Ge, S.C. Wang, Y.X. Wang, Heat-transfer film coefficients of falling film horizontal tube evaporators, *Desalination* 166 (2004) 223–230.
- [7] K.R. Chun, R.A. Seban, Heat transfer to evaporating liquid films, *ASME J. Heat Transfer* 93 (1971) 391–396.
- [8] W.H. Parken, L.S. Fletcher, J.C. Han, V. Sernas, Heat transfer through falling film evaporation and boiling on horizontal tubes, *ASME J. Heat Transfer* 112 (1990) 744–750.
- [9] M. Habert, Falling film evaporation on a tube bundle with plain and enhanced tubes (Ph.D. thesis), École Polytechnique Fédérale de Lausanne, Switzerland, 2009.
- [10] W. Nusselt, Die oberflächenkondensation des wasserdampfes, *Zeitschr. Ver. Deutsch. Ing.* 60 (1916) 541–575.
- [11] J. Mitrović, Influence of tube spacing and flow rate on heat transfer from a horizontal tube to a falling liquid film, in: *Proceedings of the 8th International Heat Transfer Conference*, San Francisco, CA, 1986, pp. 1949–1956.
- [12] G.N. Danilova, V.G. Burkin, V.A. Dyundin, Heat transfer in spray-type refrigerator evaporators, *Heat Transfer Soviet Res.* 8 (1976) 105–113.
- [13] L.H. Chien, R.H. Chen, An experimental study of falling film evaporation on horizontal tubes using R-134a, *J. Mech.* 28 (2012) 319–327.
- [14] J.C. Han, L.S. Fletcher, Falling film evaporation and boiling in circumferential and axial grooves on horizontal tubes, *Ind. Eng. Chem. Process. Des. Dev.* 24 (1985) 570–575.
- [15] J.J. Lorenz, D. Yung, A note on combined boiling and evaporation of liquid films on horizontal tubes, *ASME J. Heat Transfer* 101 (1979) 178–180.
- [16] L.H. Chien, C. Cheng, A predictive model of falling film evaporation with bubble nucleation on horizontal tubes, *HVAC&R Res* 12 (2006) 69–87.
- [17] G. Ribatski, J.R. Thome, Experimental study on the onset of local dryout in an evaporating falling film on horizontal plain tubes, *Exp. Therm. Fluid Sci.* 31 (2007) 483–493.
- [18] L.H. Chien, Y.L. Tsai, An experimental study of pool boiling and falling film vaporization on horizontal tubes in R-245fa, *Appl. Therm. Eng.* 31 (2011) 4044–4054.
- [19] W.T. Ji, C.Y. Zhao, Y.L. He, G.N. Xi, W.Q. Tao, Vapor flow effect on falling film evaporation of R134a outside horizontal tube bundle, in: *The 15th International Heat Transfer Conference*, Kyoto, Japan, 2014.
- [20] E.W. Lemmon, M.L. Huber, M.O. McLinden, Reference fluid thermodynamic and transport properties (REFPROP), Version 8.0, National Institute of Standards and Technology (NIST), 2008.
- [21] S. Yang, W. Tao, *Heat Transfer*, 4th ed., Higher Education Press, Beijing, China, 2006.

- [22] V. Gnielinski, New equations for heat and mass transfer in the turbulent flow in pipes and channels, *Int. Chem. Eng.* 16 (1976) 359–368.
- [23] S.J. Kline, F.A. McClintock, Describing uncertainties in single-sample experiments, *Mech. Eng.* 75 (1953) 3–9.
- [24] B. Cheng, W.Q. Tao, Experimental study of R-152a film condensation on single horizontal smooth tube and enhanced tubes, *ASME J. Heat Transfer* 116 (1994) 266–270.
- [25] Y.A. Cengel, A.J. Ghajar, Chapter eight: Internal forced convection, in: *Heat and Mass Transfer, Fundamentals and Applications*, McGraw-Hill, New York, 2011, p. 489.
- [26] R.L. Webb, C. Pais, Nucleate pool boiling data for five refrigerants on plain, integral-fin and enhanced tube geometries, *Int. J. Heat Mass Transf.* 35 (1992) 1893–1904.
- [27] M.G. Cooper, Saturation nucleate pool boiling—a simple correlation, *Int. Chem. Eng. Symp. Ser.* 86 (1984) 785–792.
- [28] S.A. Moeykens, Heat transfer and fluid flow in spray evaporators with application to reducing refrigerant inventory (Ph.D. thesis), Iowa State University, 1994.
- [29] Y. Fujita, M. Tsutsui, Experimental investigation of falling film evaporation on horizontal tubes, *Heat Trans. Jpn. Res.* 27 (1998) 609–618.
- [30] Z.H. Liu, J. Yi, Enhanced evaporation heat transfer of water and R-11 falling film with the roll-worked enhanced tube bundle, *Exp. Therm. Fluid Sci.* 25 (2001) 447–455.
- [31] H. Kuwahara, A. Yasukawa, W. Nakayama, T. Yanagida, Evaporative heat transfer from horizontal enhanced tubes in thin film flow, *Heat Trans. Jpn. Res.* 19 (1990) 83–97.
- [32] Y. Tan, G. Wang, S. Wang, N. Cui, An experimental research of spray falling film boiling on the second generation mechanically made porous surface tubes, in: *Proceedings of the 9th International Heat Transfer Conference*, Jerusalem, Israel, 1990, pp. 269–273.
- [33] T.B. Chang, J.S. Chiou, Spray evaporation heat transfer of R-141b on a horizontal tube bundle, *Int. J. Heat Mass Transf.* 42 (1999) 1467–1478.
- [34] M. Habert, J.R. Thome, Falling-film evaporation on tube bundle with plain and enhanced tubes: part I: experimental results, *Exp. Heat Transfer* 23 (2010) 259–280.